Nanometer-Scale Deposition of Metal Plating Using a Nanopipette Probe in Liquid Condition

Nanometer-Scale Deposition of Metal Plating Using a Nanopipette Probe in Liquid Condition

So ITO and Futoshi IWATA*

Department of Mechanical Engineering, Faculty of Engineering, Shizuoka University, Hamamatsu 432-8561, Japan

*E-mail address: tmfiwat@ipc.shizuoka.ac.jp

We describe a novel technique of a local metal plating using an atomic force microscope (AFM) with a nanopipette probe in liquid condition. A glass nanopipette, filled with $CuSO_4$ electrolyte solution, was used as the AFM probe. An electrode wire inside the electrolyte-filled nanopipette and the conductive surface of a Au-sputtered glass slide were employed as the anode and the cathode, respectively. To avoid drying of the nanopipette solution and clogging of the probe-edge aperture, the edge of the nanopipette was immersed in the same electrolyte solution in a liquid cell placed on the Au substrate. As for controlling the distance between the probe edge and the surface in the liquid, the nanopipette probe glued on a tuning fork quartz crystal resonator was vertically oscillated to use a method of frequency modulation in tapping-mode. By utilizing the probe-surface distance control during the deposition, nanometer-scale Cu dots were successfully deposited on the Au surfaces without diffusion of the deposition even in the liquid condition. This technique of local deposition in a liquid would be applicable for various fields such as the fabrication of micro/nanometer-scale devices and the arrangement of biological samples.

1. Introduction

There has been great interest in nanometer-scale fabrication techniques in the fields of micro- and nanometer-scale science and engineering. In particular, the nanometer-scale patterning of functional materials is very important for nanometer-scale engineering such as nanoelectronics and micro- and nano-electro-mechanical systems (MEMS/NEMS). As one method of nanometer-scale patterning of materials, local depositions based on scanning probe microscopes (SPMs) including a scanning tunneling microscope (STM) and an atomic force microscope (AFM) have been developed.[1-5] SPMs are highly effective tools for surface observation with nanometer-scale resolution. In addition, they can also be used for surface modification because they allow for direct scripting on a surface in a very accurate and well-controlled manner. As for the surface modification of deposition materials, we have developed local deposition using an AFM with a nanopipette probe[6-8]. A glass nanopipette probe can be filled with various types of liquid solution; therefore, various materials can be deposited on a surface through the nanopipette aperture using the interactions between the surface and the liquid solution such as electrochemical reactions[7] and electrophoresis.[8] However, during the deposition process, the aperture of the nanopipette probe often becomes clogged because of drying of the liquid inside the nanopipette owing to contact with air. Furthermore, the liquid solution often cannot contact the surface because of the air-water interface at the nanopipette aperture. These phenomena would tend to reduce the reproducibility of deposition.

These issues can be solved by the deposition in liquid condition. With regard to the SPM using a nanopipette probe in liquid condition, a scanning ion-conductance microscope (SICM)[9] is known as a type of scanning probe microscope (SPM). The SICM uses an electrolyte-filled nanopipette as the probe of the SPM. For the distance control between the probe and the surface, the SICM uses the ionic-conductance field at the edge of the nanopipette to obtain the surface topography in the electrolyte solution. The SICM has also been applied to the deposition of biological materials such as immunoglobulin G (IgG) and deoxyribonucleic acid (DNA) in liquid.[10-12] However, in depositions using an SICM, the deposited material was diffused in the liquid because of the gap of several tens of nanometers between the probe edge and the surface. Therefore, the diameters of the deposited dots

were much larger than that of the nanopipette aperture.[12)]

In this paper, we describe a novel technique of local deposition of material using an AFM with a nanopipette probe in liquid condition. As a demonstration of local deposition in liquid condition, nanometer-scale Cu metal plating was carried out in an electrolyte solution. The AFM system is used for the distance control between the probe and the surface during the deposition. In the liquid, the edge of the nanopipette probe was almost in contact with the surface to achieve a local deposition domain approximately the same size as the nanopipette aperture. By changing the distance between the probe and the surface during the deposition process, localization of the deposition domain was investigated. In addition, the reproducibility of the deposition was estimated by the deposition of a dot array.

2. Experimental Procedure

A nanopipette probe was fabricated from a capillary glass tube with a 1.0 mm outer diameter and a 0.6 mm inner diameter (Narishige) by thermal pulling using a CO_2 laser-type nanopipette puller (SUTTER; P-2000). The resultant probe had an aperture of approximately 200 nm in diameter and the outer edge of the nanopipette was approximately 300 nm in diameter.[7)]

As for the local deposition of materials in the liquid condition, Cu metal plating was employed in this experiment. Figure 1(a) shows a method of Cu dot deposition in liquid condition. A 30-μm-diameter Cu wire was inserted into the nanopipette probe as an anodic electrode for the electrochemical reaction. As a conductive substrate for the deposition, a Au surface was used as a cathodic electrode. The Au surface was prepared by vapor deposition on a Cr-evaporated glass slide. The nanopipette was filled with 0.001 M $CuSO_4$ electrolyte aqueous solution prepared using reagent-grade $CuSO_4$ (Wako). Then, a silicone rubber ring used as a liquid cell placed on the Au surface was filled with the same electrolyte solution. Cu metal-plating dots were deposited on the Au surface by immersing the edge of the nanopipette probe in the solution of the liquid cell. When a dc bias voltage was applied between the electrode wire and the Au surface, metal Cu was

electrochemically deposited on the surface as a result of the flow of an ionic current. At that time, when the distance between the edge of the nanopipette and the surface was significant, as shown in Fig. 1(b), the flow of the ionic current would be spread and the deposition domain would become much larger than the nanopipette aperture. On the other hand, when the edge of the nanopipette was almost in contact with the surface, as shown in Fig. 1(c), the flow of the ionic current would pass through only the nanopipette aperture; therefore, a Cu dot was almost deposited inside the nanopipette aperture without spreading of the ionic current because spreading of the ionic current was confined by the nanopipette. As a result, it is possible to deposit a local metal plating domain approximately the same size as the nanopipette aperture. The ionic current during the deposition process was detected with a current/voltage (*I*-*V*) converter, and then recorded using a digital storage oscilloscope.

To maintain a contact condition between the probe edge and the surface, it was necessary to control the probe-surface distance during the deposition process. As described above, the SICM detects the ionic current to control the distance between the probe and the surface. However, it is difficult for the SICM to maintain a contact condition between the probe and the surface because the flow of the ionic current was almost blocked by the nanopipette in the contact condition. Furthermore, in our previous studied, a shear-force control was employed for the probe-surface distance control.[6-8] In the shear-force control, the probe is oscillated in the lateral direction on the surface. However, it is difficult to apply the shear-force control in liquid condition because the shear-force is generated by meniscus force on a surface in air atmosphere.[13, 14] In this study, we employed a tapping-mode AFM to control the distance between the probe and the surface in the liquid condition. The nanopipette was oscillated in the vertical direction in the liquid. However, for the nanopipette, it is difficult to apply an optical-lever system[15] because the nanopipette is long and straight. To detect the oscillation of the probe, a force sensor based on a tuning fork quartz crystal resonator (TF-QCR) was used. As for the distance control, a frequency modulation AFM (FM-AFM) [16] was employed because of its high sensitivity in force detection in comparison with an amplitude

modulation AFM (AM-AFM).[16] The nanopipette probe was glued on one beam of the TF-QCR to detect the oscillation of the probe. To prevent a short circuit between the Cu electrode wire and the electrode of the TF-QCR, the nanopipette probe was fixed on the upper beam of the TF-QCR, as shown in Fig. 2(a). The TF-QCR was slightly tilted with respect to the vertical direction to avoid interference between the nanopipette probe and the lower beam of the TF-QCR. The length of the nanopipette probe was less than 4 mm. A photograph of the assembled force sensor is shown in Fig. 2(b). During the deposition, the solution in the nanopipette would be evaporated and dried. However, the nanopipette is spontaneously refilled from the solution outside the pipette owing to a capillary phenomenon since the edge of the nanopipette is immersed in the liquid solution. Therefore, the amount of solution inside the nanopipette is maintained during the deposition. The experimental configuration of the FM-AFM with a nanopipette probe is shown in Fig. 2(c). The probe was oscillated with the TF-QCR by a dither piezoelectric actuator (PZT) in the vertical direction at its resonance frequency of approximately 30 kHz. The displacement characteristic of the dither PZT was 1 nm/V. The amplitude of the probe oscillation was calculated from the frequency response of the TF-QCR sensor. Figure 3 shows the frequency response of the assembled force sensor. The applied voltage of the dither PZT was 400 mV. During the measurement of the frequency response, the edge of the nanopipette was immersed in the liquid cell filled with the electrolyte solution. In Fig. 3, the horizontal axis indicates the frequency of the oscillated dither PZT and the vertical axis indicates the calculated amplitude. The amplitude of the probe oscillation was less than 10 nm. Using a self-excited circuit (Nanosurf; easyPLL plus Controller), the probe could be kept oscillating at the resonance frequency. As the oscillating probe approached the surface, the resonance frequency shifted. The shift of the resonance frequency was detected using a phase locked loop (PLL) circuit (Nanosurf; easyPLL plus Detector). The output signal of the PLL circuit was fed into a custom-built AFM controller[17] to keep the probe-surface distance constant. In our AFM system, the nanopipette was used not only for the deposition but also for the observation of the surface. Therefore, the topographical images were sequentially obtained using the same nanopipette probe in a $CuSO_4$

aqueous solution after the deposition process.

3. Results and Discussion

Figure 4(a) shows a topographical image of a Cu dot on the Au surface deposited by the present method. The Cu dot was deposited by applying a dc bias voltage of 3.5 V for 2.5 s. During the deposition process, the set value for the frequency shift was 10 Hz. The cross-sectional profile of the deposited dot structure is shown in Fig. 4(b). The width and height of the dot structure were 198 and 28 nm, respectively. The width of the dot was approximately the same as the diameter of the nanopipette aperture. Thus, the amplitude of the oscillated probe was small enough to deposit materials on the surface without diffusion. In the depositions based on the SICM, which is a similar method using a nanopipette, the domains have been no smaller than 800 nm in diameter, owing to the diffusion of materials.[12)] In the SICM, it is difficult to maintain contact between the edge of the probe and the surface since the probe-surface distance is controlled in the non contact condition. On the other hand, in the proposed method, spreading of the ionic current was confined by the nanopipette because the AFM-based distance control allowed deposition of the materials in the contact condition. Therefore, an aperture-size deposition domain was achieved in the liquid condition.

The width and height of the deposited dots were investigated by changing the set value for the frequency shift during the deposition process. In our FM-AFM system, the probe-surface distance was controlled according to the size of the resonance-frequency shift. By changing the set value for the frequency shift, it was possible to adjust the probe-surface distance. Figure 5(a) indicates the frequency shift as a function of displacement of the probe-surface distance on a Au surface in $CuSO_4$ liquid solution. In Fig. 5(a), the horizontal axis indicates the displacement of the probe-surface distance. As the edge of the probe approached the surface, the size of the resonance-frequency shift increased. The zero-point in the horizontal axis is defined the start point of increasing the shift of the resonance frequency. Cu dots were deposited by changing the set value for the frequency shift. The set values for the frequency shift were 5, 10, and 15 Hz. As for the observation of the dot structures,

the set value for the frequency shift was 5 Hz. The displacement of the probe-surface distance was calculated from Fig. 5(a). In the case of the set value of 10 Hz, the probe-surface distance was 6 nm smaller than that in the case of the set value of 5 Hz. Similarly, in the case of the set value of 15 Hz, the probe-surface distance was 11 nm smaller than that in the case of the set value of 5 Hz. All the depositions were carried out using the same nanopipette probe with a bias voltage of 3.5 V and 2 s. Figures 5(b) and 5(c) show the typical topographical images of the deposited dot structures. Cross-sectional profiles of these deposited dots are shown in Figs. 5(d) and 5(e). Figures 5(f) and 5(g) show the width and height of the deposited Cu dots as a function of the frequency shift during the deposition process, respectively. The width of the deposited Cu dots significantly decreased with increases in the frequency shift. On the other hand, the height of the deposited dots decreased slightly by increasing the set value of the frequency shift. The decrease in the width indicates that the deposition domain was localized by approaching the edge of the nanopipette. The ionic current was passed through only the nanopipette aperture; as a result, the spreading of the ionic current would be confined by the nanopipette probe. Therefore, by utilizing a precision probe-surface distance control based on the FM-AFM technique, even if deposition is carried out in liquid condition, it is possible to deposit a Cu metal-plating dot that is approximately the same size as the nanopipette aperture.

Dot array deposition was carried out to estimate the reproducibility of the deposition. Figure 6(a) shows a topographical image of Cu dots sequentially deposited in liquid condition. In this experiment, every dot was deposited with the same bias voltage and deposition time of 3.5 V and 3 s, respectively. The set value for the frequency shift was 10 Hz. Figure 6(b) shows the cross-sectional profile of the dots shown in Fig. 6(a). The average width and height of the six deposited dots were 272 and 25 nm, respectively. The deposited dots were formed with an asymmetric shape. This asymmetric shape might be caused by the gradient of the probe edge between the surface and the edge of the probe. In this study, the nanopipette was glued on one beam of the TF-QCR vertically with respect to the surface. However, it was difficult to adjust the gradient of the nanopipette probe precisely because the probe and the force sensor did not have an adjustment mechanism such as a tilting stage. To

control the gradient between the probe and the surface precisely, a tilting stage will be installed into the probe holder of the AFM system in a future apparatus. The average volume, calculated from the topographical images using image processing software (Image Metrology A/S; SPIP), was 2.37×10^{-21} m^3. The volume of the maximum deposited dot is 15% larger than that of the minimum one. In our previous research of local deposition in air atmosphere, the volume of the maximum dot was 310% larger than that of minimum one.[18] According to Faraday's law of electrolysis, the volume of a deposited Cu dot increases in proportion to the electric charge during the deposition. The dispersion of the electric charge causes the difference in the deposited volume. In the air atmosphere, a Cu dot was deposited on the surface by forming a meniscus between the edge of the probe and the surface. However, the meniscus was unstable in the air atmosphere because of various reasons such as the roughness of the surface, the differences in local surface resistance, and the variation of surface energy. Therefore, the flow of the ionic current was unstable during the deposition. As a result, the volume of the deposited dots was not constant in each deposition. On the other hand, in a liquid condition, the electrical path of an ionic current between the probe and the surface is stable owing to the liquid environment surrounding the nanopipette. Figure 6(c) shows the behavior of the ionic current during the deposition in the liquid. The average of six electric charges was 136.3 pC. The difference between the maximum and minimum values among the six electric charges was 0.6 pC, corresponding to 0.4% of the average electric charge. In the liquid-condition deposition, the flow of the ionic current became stable in comparison with the case in air; therefore, the volume of deposition became constant in each deposition process.

In respect of the deposition using the SPM in liquid condition, more smaller metal depositions on the conductive surface were demonstrated by STM tips using electrochemical reactions.[19-22] However, the STM cannot be used for the observation of insulating materials because the STM uses a tunneling current for the distance control between the tip and the surface. Therefore, it is difficult for the STM to observe the structures on insulating materials such as an oxide structure patterned by the electrochemical reactions.[22, 23] On the other hand, the proposed AFM system can observe the

surface of the insulating materials in liquid condition. The nanopipette would be applicable for the deposition and observation of the insulating materials in liquid condition using the same probe. Utilizing the probe-surface distance control based on the FM-AFM allows an aperture-size deposition domain in liquid condition without spreading of the ionic current. Furthermore, the nanopipette probe can also be filled with various types of liquid solution such as colloidal solutions and insulating materials. Therefore, the deposition and the observation of various types of material would be expected using the nanopipette probe in liquid condition. This technique of local deposition could be applied to various fields such as nanometer-scale science, engineering, and in particular, biological fields since it can be used in liquid condition.

4. Conclusions

Local deposition of Cu metal plating in liquid condition was carried out using an AFM with a nanopipette probe. During the deposition process, the probe-surface distance control based on FM-AFM allowed for a local deposition domain that was approximately the same size as the nanopipette aperture, without spreading of the ionic current in liquid condition. As for the sequential deposition of Cu dots, the ratio of the dispersion of the electric charge to the average value was 0.4%. This results in a constant deposition volume for each deposition process. Since the nanopipette can be filled with various types of material, this technique of local deposition in the liquid condition is expected to be applicable to various fields, such as the nanometer-scale fabrication of nanodevices and nanobiological fields.

Acknowledgements

This work was partly supported by the Knowledge Cluster Initiative of the Ministry of Education, Culture, Sports, Science and Technology of Japan (MEXT). The authors would like to acknowledge Grant-in-Aid for Scientific Research from MEXT and CREST of the Japan Science and Technology Agency (JST).

1) R. D. Piner, J. Zhu, F. Xu, S. Hong, and C. A. Mirkin: Science **283** (1999) 661.

2) S. H. Hong and C. A. Mirkin: Science **288** (2000) 1808.

3) Y. Li, B. W. Maynor, and J. Liu: J. Am. Chem. Soc. **123** (2001) 2105.

4) K. Kaisei, K. Kobayashi, K. Matsushige, and H. Yamada: Jpn. J. Appl. Phys. **49** (2010) 06GH02.

5) H. J. Mamin, P. H. Guether, and D. Rugar: Phys. Rev. Lett. **65** (1990) 2418.

6) F. Iwata, Y. Sumiya, S. Nagami, and A. Sasaki: Nanotechnology **15** (2004) 422.

7) F. Iwata, Y. Sumiya, and A. Sasaki: Jpn. J. Appl. Phys. **43** (2004) 4482.

8) F. Iwata, Y. Sumiya, S. Nagami, and A. Sasaki: Nanotechnology **18** (2007) 105301.

9) P. K. Hansma, B. Drake, O. Marti, S. A. C. Gould, and C. B. Prater: Science **243** (1989) 641.

10) A. Bruckbauer, L. Ying, A. M. Rothery, D. Zhou, A. I. Shevchuk, C. Abell, Y. E. Korchev, and D. Klenerman: J. Am. Chem. Soc. **124** (2002) 8811.

11) A. Bruckbauer, D. Zhou, L. Ying, Y. E. Korchev, C. Abell, and D. Klenerman: J. Am. Chem. Soc. **125** (2003) 9835.

12) K. T. Rodolfa, A. Bruckbauer, D. Zhou, Y. E. Korchev, and D. Klenerman: Angew. Chem. Int. Ed. **44** (2005) 6854.

13) M. Antognozzi, A. D. L. Humphris, and M. J. Miles: Appl. Phys. Lett. **78** (2001) 300.

14) M. A. D. Roby and G. C. Wetsel, Jr.: Appl. Phys. Lett. **69** (1996) 3689.

15) G. Meyer and N. M. Amer: Appl. Phys. Lett. **53** (1988) 1045.

16) T. R. Albrecht, P. Grütter, D. Horne, and D. Rugar: J. Appl. Phys. **69** (1991) 668.

17) A. Sasaki, F. Iwata, A. Katsumata, and J. Fujiyasu: Rev. Sci. Instrum. **68** (1997) 1296.

18) S. Ito, T. Keino, and F. Iwata: Jpn. J. Appl. Phys. **49** (2010) 08LB16.

19) W. Li, A. Virtanen, and M. Penner: J. Phys. Chem. **96** (1992) 6529.

20) D. M. Kolb, R. Ullmann, and T. Will: Science **275** (1997) 1097.

21) D. M. Kolb and F. C. Simeone: Electrochim. Acta. **50** (2005) 2989.

22) H. Sugimura and N. Nakagiri: J. Vac. Sci. Technol. A **14** (1996) 1223.

23) W. C. Moon, T. Yoshinobu, and H. Iwasaki: Jpn. J. Appl. Phys. **41** (2002) 4754.

Fig. 1. (Color Online) Schematics of the deposition using a nanopipette probe in the liquid. (a) Nanopipette was filled with $CuSO_4$ electrolyte aqueous solution. The same electrolyte solution was filled in a liquid cell. A Cu metal-plating dot was deposited while applying a dc bias voltage between the electrode wire and the Au surface. (b) As the edge of the nanopipette does not contact the surface, the flow of the ionic current is spread in the liquid. The deposition domain became much larger than the diameter of the nanopipette aperture. (c) As the edge of the nanopipette comes into contact with the surface, the Cu dot is deposited inside of the nanopipette aperture. The width of the deposited dot would be approximately the same size as the diameter of the nanopipette aperture.

Fig. 2. (Color Online) Schematic diagram of the experimental configuration of the FM-AFM using a nanopipette probe. (a) Schematic diagram of a force sensor using a TF-QCR. The TF-QCR was slightly tilted with respect to the vertical direction. (b) Photograph of the assembled force sensor using a TF-QCR. A Cu wire was inserted into the nanopipette, and then the nanopipette was fixed on the upper beam of the TF-QCR to prevent short circuit between the Cu wire and the electrode of the TF-QCR. (b) Experimental set up of the FM-AFM using the nanopipette probe. The edge of the nanopipette was immersed in the liquid cell filled with $CuSO_4$ electrolyte aqueous solution. The probe and the TF-QCR were oscillated of its resonance frequency. The shift of the resonance frequency was detected using a PLL circuit to maintain the probe-surface distance.

Fig. 3. (Color Online) Frequency response of the assembled force sensor in $CuSO_4$ electrolyte aqueous solution.

Fig. 4. (Color Online) Topographical image of Cu metal plating dot on Au surface. (a) Cu metal plating dot with an applied voltage of 3.5 V for 2 s. The set value for the frequency shift was 10 Hz during the deposition. (b) Cross-sectional profile of the dot structure in image (a).

Fig. 5. (Color Online) (a) Frequency shift-distance curve measured on Au surface in $CuSO_4$ aqueous solution. The resonance frequency of the probe was 30.5 kHz. The zero-point in the horizontal axis is defined as the start point of increasing the shift of the resonance frequency. (b) Topographical image of the deposited Cu dot with a set value for the frequency shift of 5 Hz. (c) Topographical image of the deposited Cu dot with a set value for the frequency shift of 15 Hz. (d) Cross-sectional profile of the deposited Cu dot in image (b). (e) Cross-sectional profile of the deposited Cu dot in image (c). (f) Width of the deposited dots as a function of the set value for the frequency shift. (g) Height of the deposited dots as a function of the set value for the frequency shift. All the dots were deposited using the same nanopipette probe with an applied voltage of 3.5 V for 2 s.

Fig. 6. (Color Online) Array of dots continuously deposited in liquid condition. (a) Topographical image of dot array on the surface. Roman numerals indicate the sequence of the deposition. All the dots were deposited with an applied voltage of 3.5 V for 3 s. (b) Cross-sectional profile of the deposited Cu dots. (c) Behavior of the ionic current between the Cu electrode wire and the surface during the deposition. The number above each peak indicates the electric charge calculated from the ionic current during the deposition process.

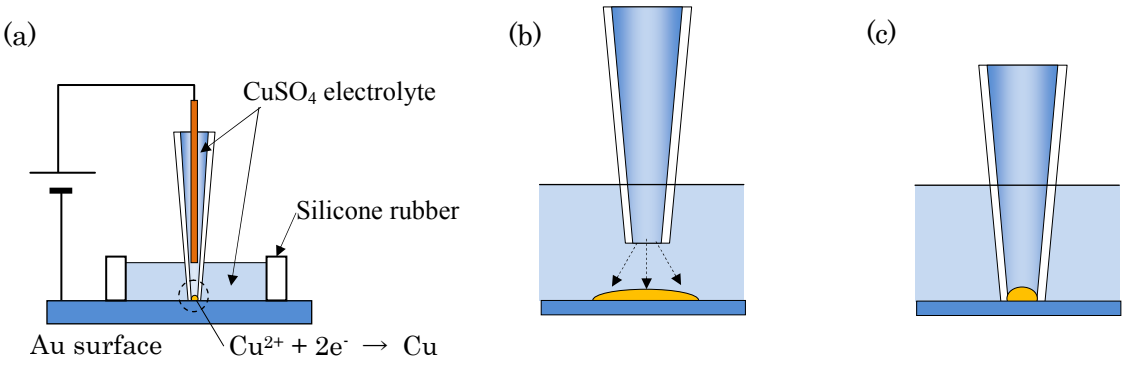

Fig. 1 So ITO

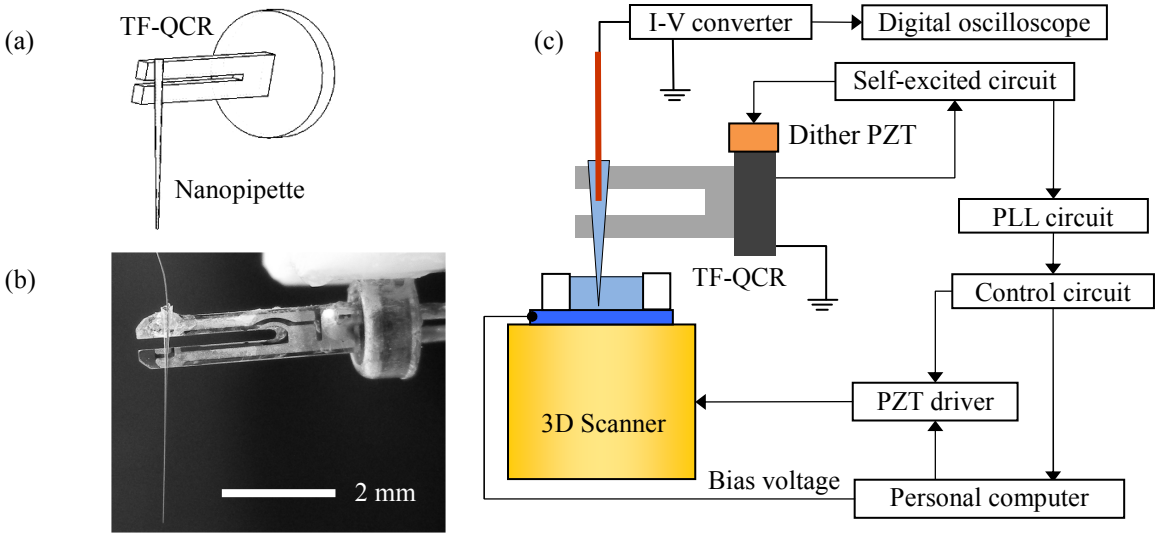
(a)
TF-QCR
Nanopipette
(b)
2 mm
(c)
I-V converter
Digital oscilloscope
Self-excited circuit
Dither PZT
PLL circuit
TF-QCR
Control circuit
3D Scanner
PZT driver
Bias voltage
Personal computer

Fig. 2 So ITO

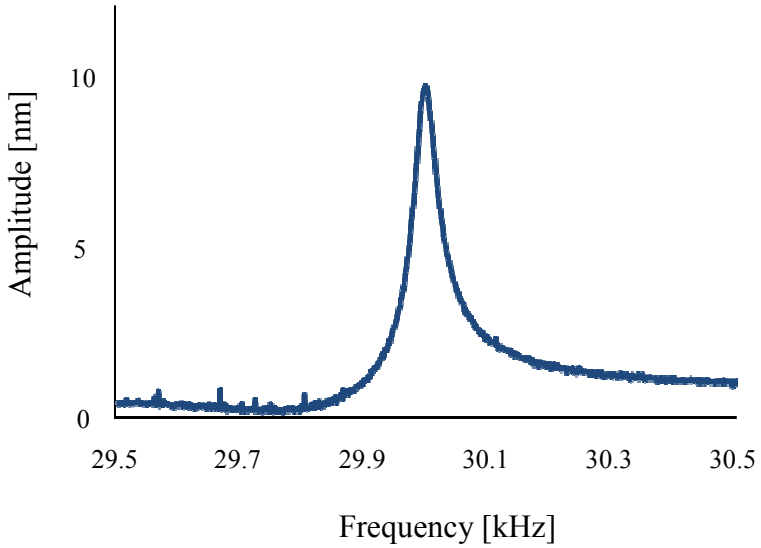

Fig. 3 So ITO

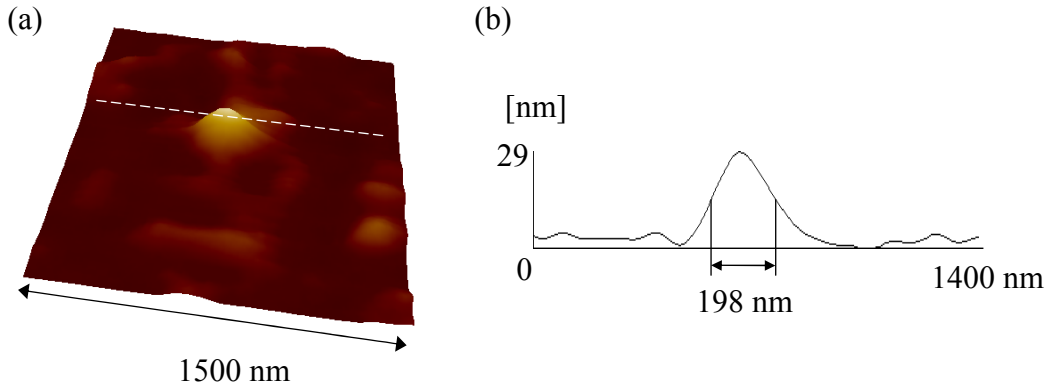

Fig. 4 So ITO

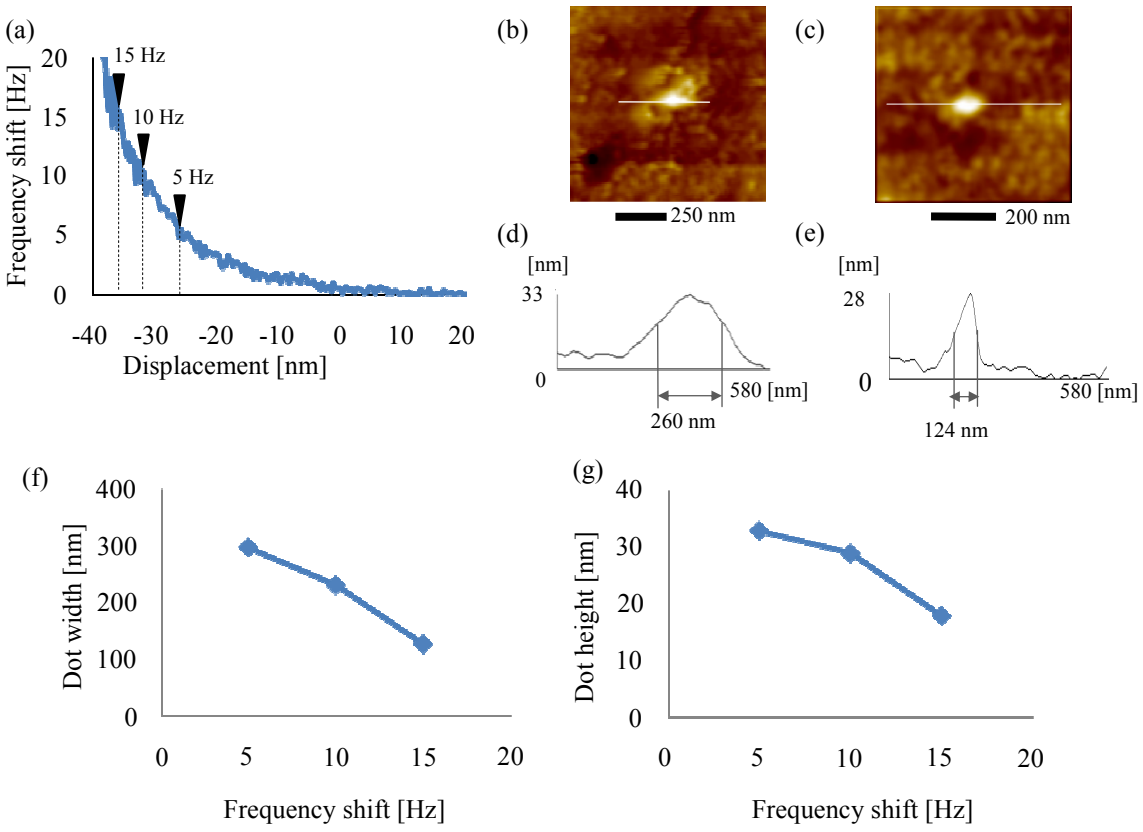
(a)
15 Hz
10 Hz
5 Hz
Frequency shift [Hz]
20
15
10
5
0
-40 -30 -20 -10 0 10 20
Displacement [nm]
(b)
250 nm
(c)
200 nm
(d)
[nm]
33
0
580 [nm]
260 nm
(e)
[nm]
28
0
580 [nm]
124 nm
(f)
Dot width [nm]
400
300
200
100
0
0 5 10 15 20
Frequency shift [Hz]
(g)
Dot height [nm]
40
30
20
10
0
0 5 10 15 20
Frequency shift [Hz]

Fig. 5 So ITO

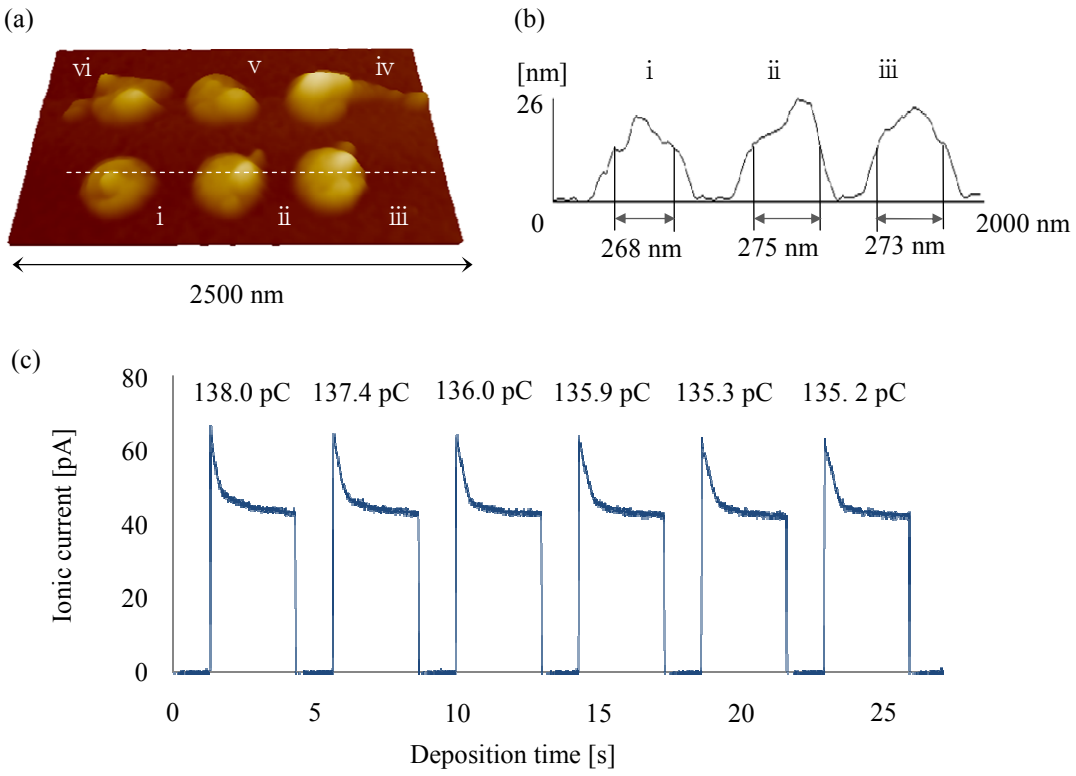
(a)
vi
v
iv
i
ii
iii
2500 nm
(b)
[nm]
i
ii
iii
26
0
268 nm
275 nm
273 nm
2000 nm
(c)
138.0 pC
137.4 pC
136.0 pC
135.9 pC
135.3 pC
135. 2 pC
Ionic current [pA]
80
60
40
20
0
0
5
10
15
20
25
Deposition time [s]

Fig. 6 So ITO